Supporting information

Supplemental Figures

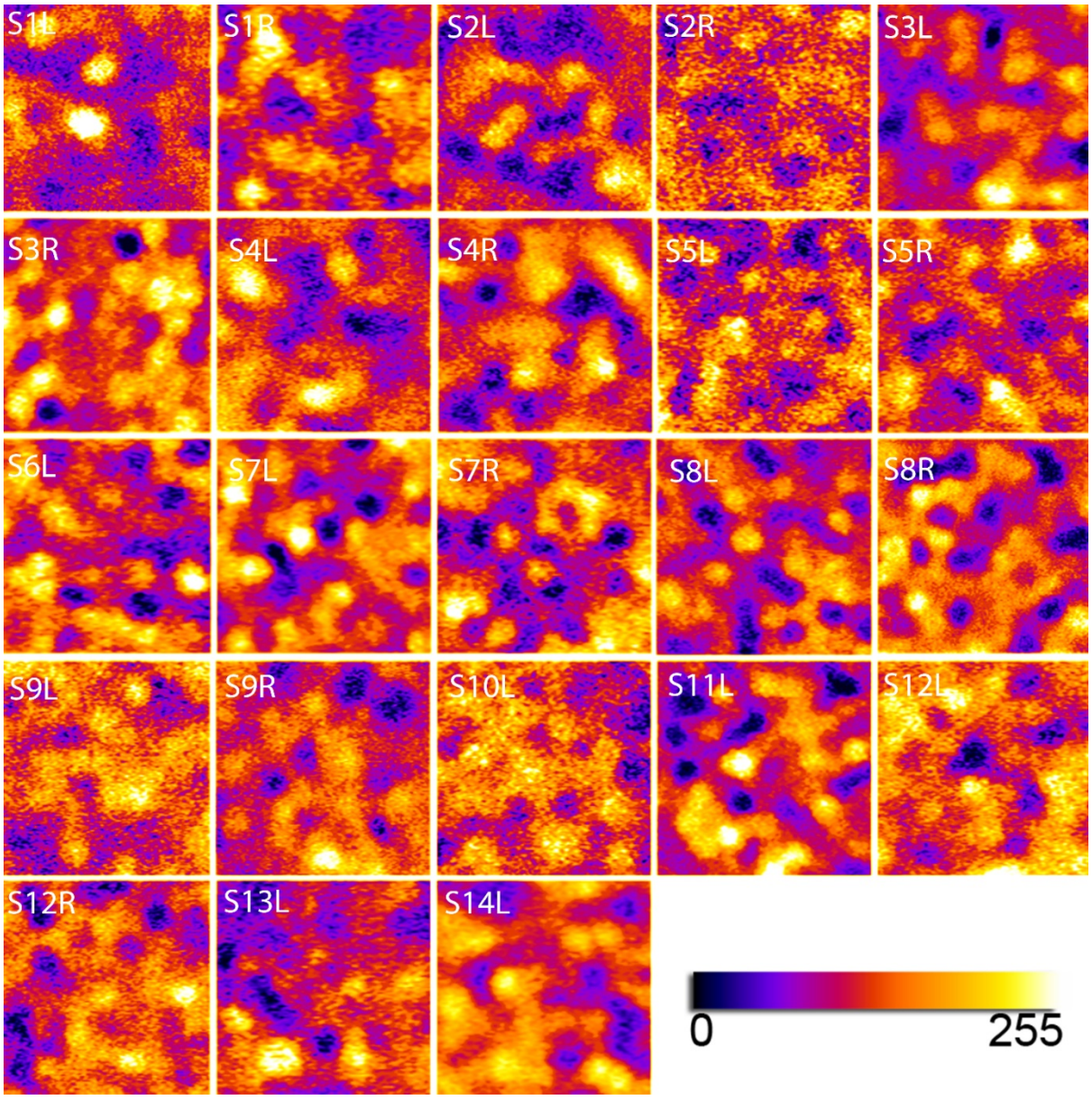

Figure S1 – AO-ICG ROIs from the foveal center as shown in **Figure 1** but displayed using a heatmap based on signal intensity in each pixel measured over a dynamic range of 0-255. Subject codes are indicated (**Table S1**) (L=left eye, R=right eye). The histogram of fluorescence intensities corresponding to these images is shown in **Figure S2.** All images are 100 µm x 100 µm.

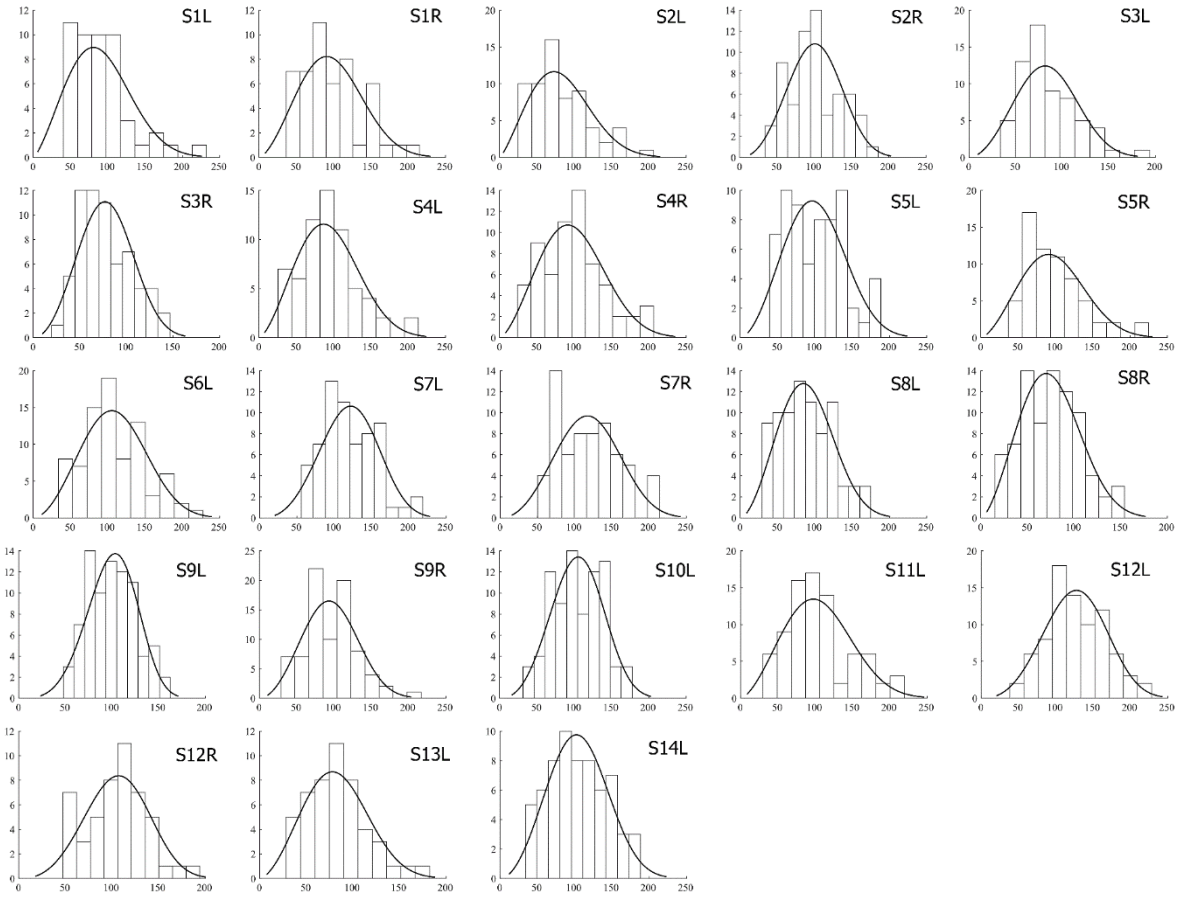

Figure S2 – Distribution of ICG fluorescence intensities from automated segmentation of RPE cells in the ROIs shown in **Figure 1**. X-axis indicates ICG fluorescence intensity while y-axis indicates counts. The distribution of fluorescence does not appear to be bimodal across the subjects. The combined data across all subjects is shown in **Figure 1E**.

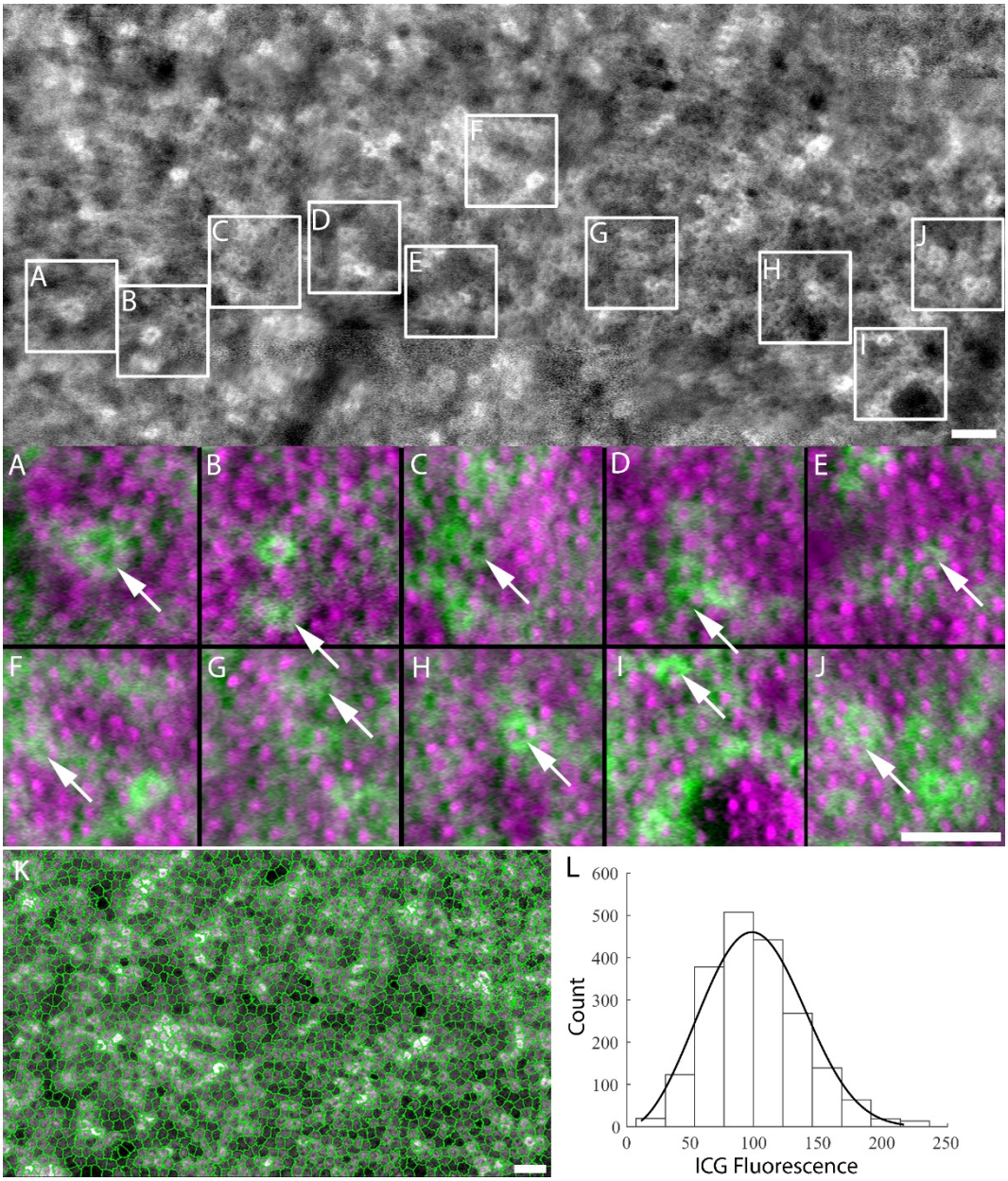

Figure S3 – Eccentric AO-ICG RPE signal with similar heterogeneity observed (subject S10L, retinal eccentricity: 3.9 to 5.0 mm temporal). Eccentric RPE cells are slightly larger compared to foveal RPE cells, enabling individual RPE cell nuclei to be observed directly in the human eye (hypofluorescent dark centers). Dark lines are due to overlying blood vessels. (A-J) Zooms of AO-ICG signal (green) merged with simultaneously-acquired, registered split detection images of presumed cone photoreceptor inner segments (magenta), showing that the observed RPE nuclei (e.g. arrows) are not an artifact of cone "imprinting" (3). (K) Automated superpixel segmentation of RPE cells and (L) corresponding distribution of RPE fluorescence intensities (left axis). There was no significant difference between fluorescence distributions of eccentric and foveal RPE cells (n=1,399 foveal cells, 1975 eccentric cells, p=0.06, Kruskal-Wallis ANOVA). Black line, fit to Weibull distribution. All scale bars, 50 μm.

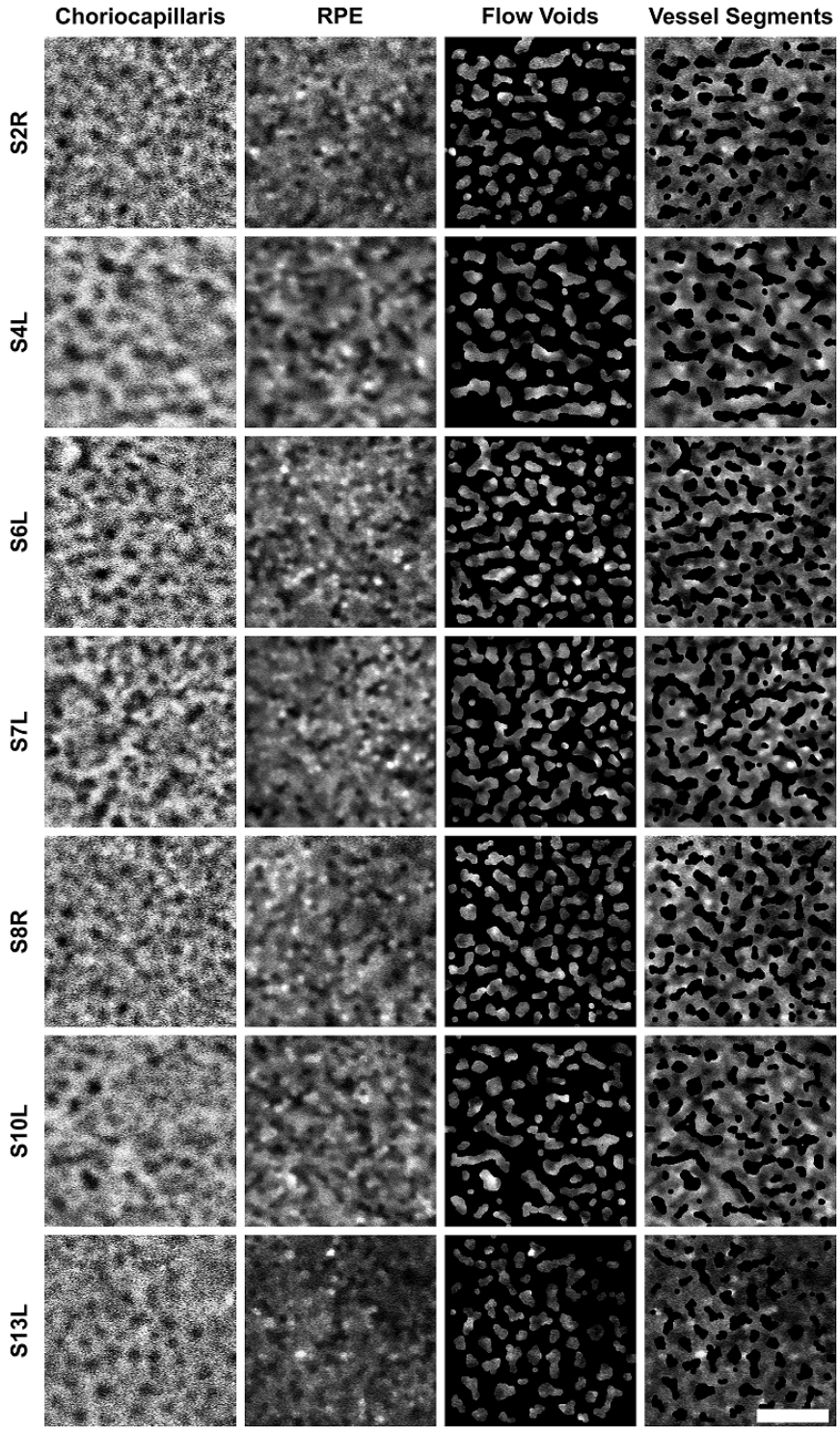

Figure S4 – Comparison of the heterogeneous AO-ICG RPE pattern to the underlying choriocapillaris, as revealed by AO-ICG (*in vivo* human imaging). (from left to right) Image of choriocapillaris; AO-ICG RPE pattern, co-registered to the choriocapillaris image; AO-ICG signal of RPE cells residing above manually-segmented flow voids; AO-ICG signal of RPE cells residing above choriocapillaris vessel segments. ICG fluorescence in RPE cells above flow voids was higher compared to ICG fluorescence in RPE cells above vessels ($p<0.05$, two tailed paired t-test). Scale bar, 150 μm.

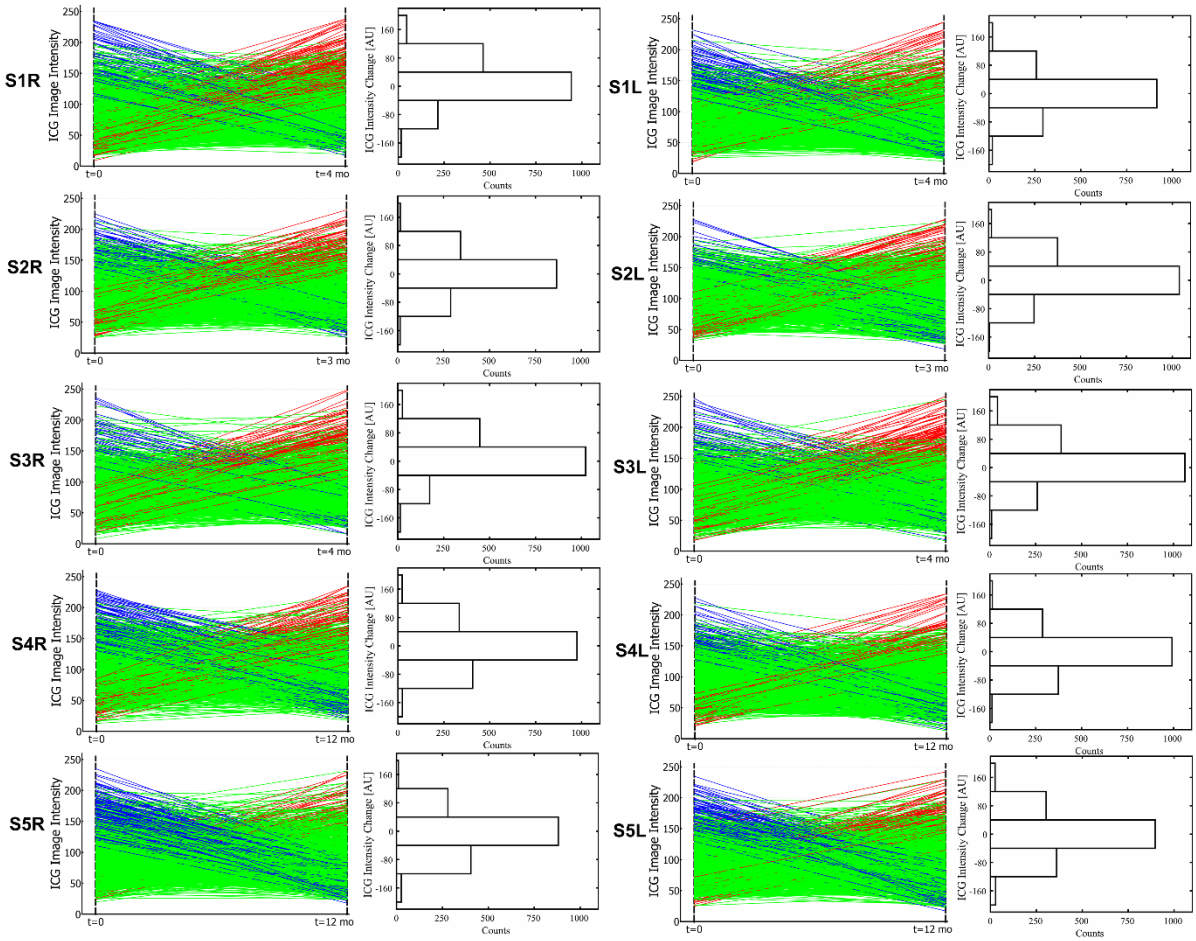

Figure S5 – Longitudinal change in AO-ICG fluorescence of all tracked cells corresponding to the data shown in **Figure 4**. For each subject, the cell-by-cell change between the two visits is shown, where green lines indicate no detected change, red denotes increase in fluorescence, and blue, decrease. The distribution of changes is shown to the right.

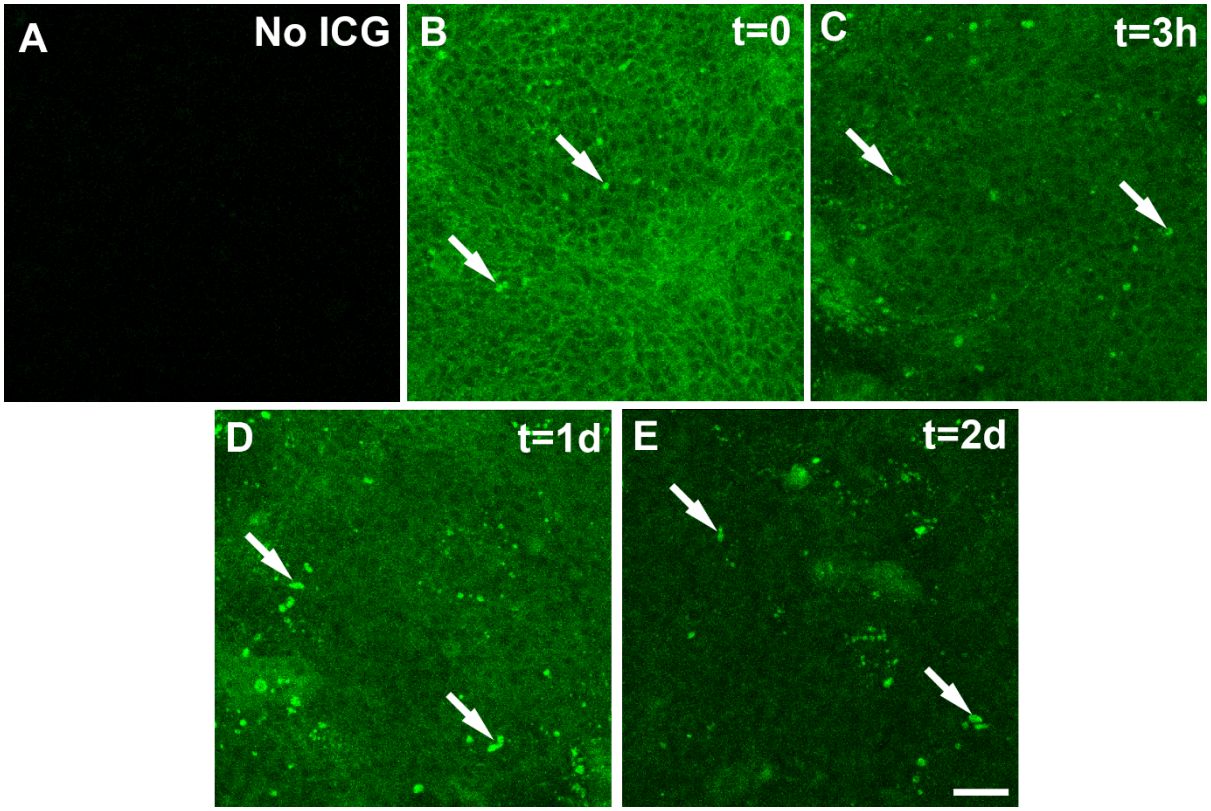

Figure S6 – Time series of ICG uptake and clearance in iPSC-RPE cells derived from individuals with oculocutaneous albinism type, imaged on a custom confocal microscope outfitted with near-infrared excitation and emission capabilities. The time (0, 3 hours, 1 day, 2 days) denotes the time elapsed after ICG was washed out from the culture media. Arrows denote artifacts likely due to clumping of ICG. Scale bar, 40 μm.

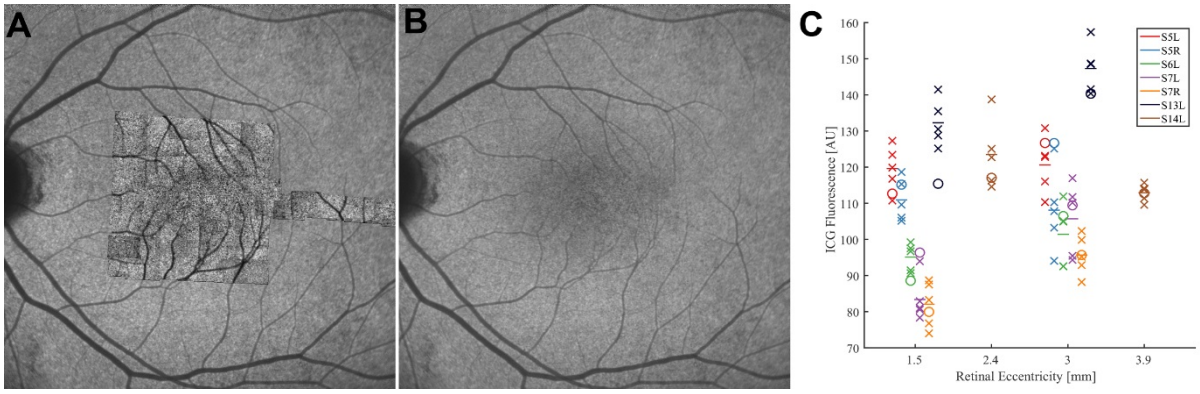

Figure S7 – Montage of overlapping AO-ICG images (A) overlaid on a conventional ICG image (Spectralis HRA+OCT, Heidelberg Engineering, Heidelberg, Germany). (B) The Spectralis image was acquired immediately after AO-ICG imaging was complete. The ICG fluorescence is dependent on the retinal eccentricity and is normally less fluorescent in the fovea when compared to non foveal regions, with the exception of blood cells and the optic nerve head. (C) There is no apparent difference in ICG fluorescence in areas that have been imaged using AO-ICG. Comparison of ICG fluorescence in eccentricity-matched regions that either had AO imaging performed (x) or did not have AO imaging performed (o) revealed no difference in fluorescence intensity due to AO imaging ($p=0.45$, one-tailed paired t-test). This data suggests that AO-ICG imaging does not cause any detectable bleaching of the ICG fluorescence.

Supplemental Tables

Table S1 – Subject information

Subject	Eye	Visit description[1]	Age	Sex	Race
S1	OU	B, R4	33	M	Caucasian
S2	OU	B, R3, CC	25	F	Caucasian
S3	OU	B, R4	47	F	African-descent
S4	OU	B, F2[2], R12+TTS, CC	27	M	Caucasian
S5	OU	B, F4, R12	42	F	Caucasian
S6	OS	B+TTS, CC	42	M	Hispanic
S7	OU	B+TTS, CC	24	F	Caucasian
S8	OU	B, CC	40	F	Caucasian
S9	OU	B	35	M	Asian
S10	OS	B+TTS+IRAF+E, CC	21	F	Hispanic
S11	OS	B+E	24	F	African-descent
S12	OU	B	39	F	Hispanic
S13	OS	B+TTS[3], CC	52	F	African-descent
S14	OS	B+IRAF	35	F	Hispanic

[1] B: baseline (or single) visit; F#: follow up imaging (no repeated injection), # days afterwards; R#: repeat visit with new injection, # months afterwards; TTS: time to stability, images recorded every minute for the first 9-10 minutes following ICG injection; IRAF: AO-IRAF images (larger detection pinhole) were taken prior to ICG administration; E: eccentric late-phase AO-ICG images acquired; CC: choriocapillaris imaging performed for comparison to overlying RPE cells.

[2] Only OS was imaged on the follow up 2 days after baseline.

[3] TTS was attempted, but subject was only able to complete minutes 0-3 and 8-9; due to insufficient data, this subject was excluded from the TTS analysis.

Table S2 – Comparison of AO-ICG RPE signal above choriocapillaris segments and above flow voids

Subject	Vessel segments	Flow voids
S2L	87.8	102.6
S4L	93.2	91.0
S6L	94.0	93.5
S7L	85.4	93.5
S8R	91.3	94.6
S10L	87.3	97.0
S13L	59.6	65.8

Table S3 – Patient information

Subject	Disease	Gene	Age	Sex
P1	Oculocutaneous Albinism	*OCA1*	25	F
P2	Oculocutaneous Albinism	*OCA1*	54	F
P3	Oculocutaneous Albinism	*OCA1*	31	M
P4	Oculocutaneous Albinism	*OCA1*	47	M
P5	Bietti Crystalline Dystrophy	*CYP4V2*	42	F
P6	Late-onset Retinal Degeneration	*C1QTNF5*	55	M

Table S4 – RPE spacing measurements across multiple visits [μm]

Subject	Visit 1	Visit 2	Absolute Change
S1L	15.2	14.2	6.6%
S1R	15.6	14.5	7.1%
S2L	14.5	15.2	4.8%
S2R	15.2	16.6	9.2%
S4L	14.2	14.5	2.1%
S4R	15.2	16.6	9.2%
P5R	22.9	25.8	12.7%
P6L	14.2	14.2	0.0%

RPE spacing [μm] was measured across two visits in a pair of co-registered AO-ICG ROIs.

Table S5 – Evaluation of whether AO-ICG bleaches the ICG fluorescence signal

Subject	Retinal Eccentricity	No AO	AO
S5L	1.5	119.6	112.7
	3	120.6	126.7
S5R	1.5	111.0	115.1
	3	108.1	126.7
S6L	1.5	95.1	88.6
	3	101.4	106.5
S7L	1.5	83.4	96.4
	3	105.7	109.4
S7R	1.5	82.1	80.0
	3	95.7	95.7
S13L	1.5	132.3	115.4
	3	147.3	140.3
S14L	2.4	123.5	117.1
	3.9	112.9	112.8

Direct comparison of ICG fluorescence values measured in eccentricity-matched areas with and without AO images taken showed no apparent difference in intensity ($p=0.45$, one-tailed paired t-test). ICG fluorescence is eccentricity dependent. Retinal eccentricity is reported in mm, and “No AO” and “AO” refer to ICG fluorescence values [AU] in locations where no AO imaging was performed and in areas where AO imaging was performed.

Supplemental Videos

Video S1 – Dynamic evolution of AO-ICG fluorescence in RPE cells following systemic injection in subject 7R, corresponding to **Figure 2A**. The simultaneously-acquired confocal reflectance channel was used to register images across timepoints.

Video S2 – Colocalization of melanin and IRAF seen with a z-stack (3.00 μm step sizes) in live induced-pluripotent stem cell-derived RPE cells from a pigmented human donor, corresponding to **Figure 3E-G**.